Airdrop Sequence Simulation using LS-DYNA® ICFD Solver and FSI Coupling

Morgan Le Garrec[1], Matthieu Seulin[1], Vincent Lapoujade[1]
[1]*DynaS+, Toulouse, France*

Abstract

DynaS+ is a French, Spanish and Portuguese distributor of LS-DYNA. It was awarded a RAPID financing by the French government for project Paraflu. This project objective is to simulate a complete airdrop sequence, including three main phases:

i) the payload freefall;
ii) the parachute deployment;
iii) the deployed phase with the payload descending under the canopy.

In this framework, the payload freefall is considered for the present paper, from the airplane cargo bay up until the initiation of parachute deployment. The LS-DYNA simulations include multi-physics and fluid-structure interaction coupling. The currently developed ICFD solver is used in conjunction with the non-linear dynamic structural solver.

The fluid domain includes the external shape of the airplane and the ramp in order to simulate the actual flow surrounding the payload during its exit.

For an accurate representation of the payload movement at the beginning of the freefall phase, initial conditions and contact management need to be representative of the physical phenomena involved. Challenges arise with ICFD meshing, as the fluid volume needs to surround the payload. This is dealt with a contact thickness between the payload and the ramp in order to keep a small fluid layer at this location.

A sensitivity analysis on turbulence models and payload weight and shape is performed. It includes a qualitative comparison between both RANS and LES models, as well as between various boundary layer mesh sizes. Aerodynamic loads exerting on the payload are computed and compared to drag and lift databases. Computer time is optimized in a manageable way for reasonable cluster usage.

The consolidated methodology is used for test cases adapted from the literature. The results are compared for validation purpose.

Introduction

The main goal of military airdrops is the accurate delivery of cargo released from a moving air vehicle via parachute. The airdrop trajectory results from the movement of the dropped package and the dynamics of the parachutes deployment (Figure 1). Although multi-physics modelling is now being used to analyze the flow around inflated parachute canopies [1][2], very little has been done in the area of payload aerodynamics [3][4].

Additional complexity ensues due to the fact that there are many different dynamic regimes characterizing the flow around the parachute and payload during a typical airdrop operation, i.e.:

i) ramp roll-out and tip-over;
ii) freefall prior to and during parachute deployment;
iii) descent and landing under a fully inflated canopy.

The payload undergoes translation, rotation and combination of both, for Reynolds numbers ranging from 10^4 to 10^6.

This paper follows the work of Michel et al.[8] and uses its conclusions to take the matter one step further. Previous work focused on the capabilities of the ICFD solver in stationary and nonstationary flows and permitted to show that the loads predictions were in agreement with the literature. In particular, the remeshing performance with moving and rotating objects was studied.

Exhaustive sensitivity analyses on the mesh and domain sizes were performed and permitted to conclude on slightly less conservative criteria than generally recommended, mostly due to the global nature of the observed phenomena.

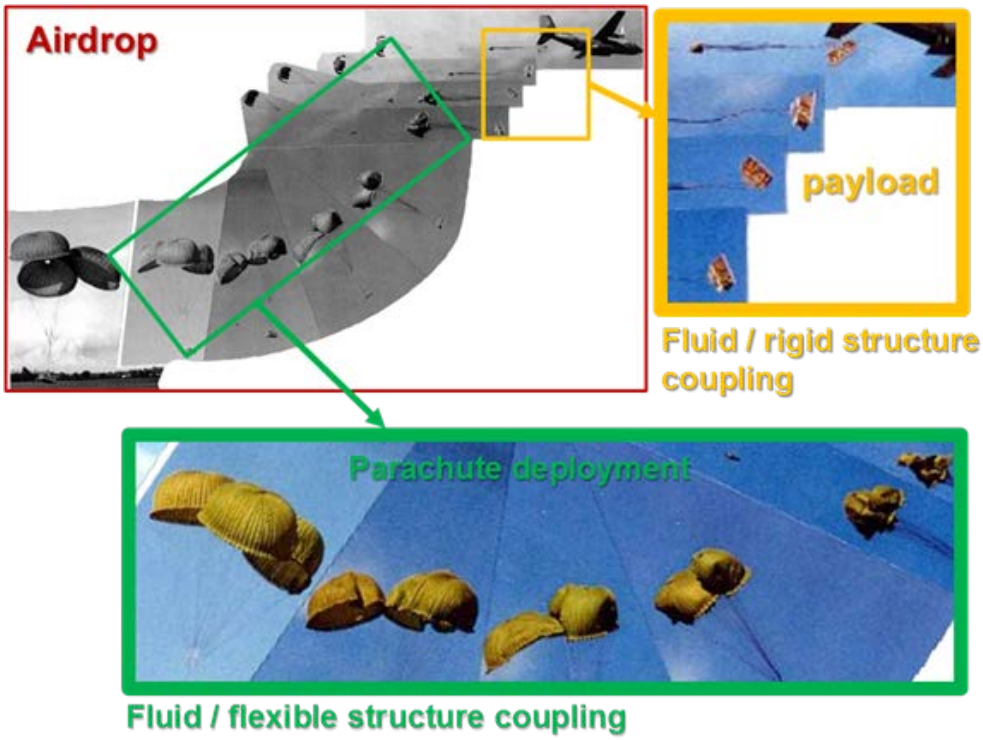

Figure 1: Highlighting of two types of fluid-structure interactions during airdrop

Objectives

The objective of this paper is to show the ICFD capabilities to model more operational problems than previously considered for airdrop applications. The freefall of rigid objects in a non-uniform air flow is considered. Several freefall cases are presented with increasing complexity, from a sphere in a steady fluid to a payload ejected from a plane with a constant velocity. For the latter, the structural model interaction with the exit ramp is accurately modelled in order to initiate the object rotation.

From a computational point of view, these cases show the ICFD mesher robustness and new mesh refinement options. Finally, the trajectories are compared to wind tunnel tests ones in order to validate the accuracy of the involved aerodynamic loads.

Preliminaries: calibration of structural properties

Before considering the immersion of a structure into an ICFD domain, the robustness of various structural modelling assumptions needs to be verified. For the present case, tuning of contact between the payload and the exit ramp is of importance.

First, it drives the maximum acceptable structural time step; as there are no deformable parts in the model, no Courant-Friedrich-Levy time step is computed and the user is free to impose the calculation time step; however, contact instabilities can be observed when choosing too large time steps. For the cases presented in this paper, a time step of 1ms is considered.

Second, the payload tipping at the exit ramp extremity involves contact on a sharp edge. This is managed thanks to the SOFT=2 formulation and a DEPTH=3 parameter enabling to deal with edge to surface contacts.

In addition to the contact definition, the ejection loading is applied by setting a velocity in the ejection direction. This is particularly convenient for implicit calculations, in order to save time in the convergence loops.

First freefall calculations with ICFD

As a preliminary model, a simple sphere falling in a still air domain without initial velocity was considered. Only qualitative observations are made at this stage.

The model is comprised of a structural rigid body with a ball shape. Its diameter is 1m and its tetrahedron mesh size is 50mm. Its mass is 5kg.

The ball external surface is extracted and used as an ICFD domain surface. The domain is further closed by a cylindrical shape. The cylinder has a height of 3m above the sphere original position and 10m below, and its diameter is 10m. The mesh size on the external frontiers is 0.5m. A spherical refinement zone is defined with a mesh size of 50mm. This zone is linked to the sphere in order to follow its movements. Finally, a non-slip boundary condition is applied to the sphere, a free-slip boundary condition is applied to the vertical cylindrical wall, a null velocity is applied to the lower cylindrical base, and a null pressure is applied to the upper cylindrical base. The air properties are:

$$\rho_{air} = 1.225\ kg.m^{-3}$$
$$\mu_{air} = 1.78 \times 10^{-5} Pa.s$$

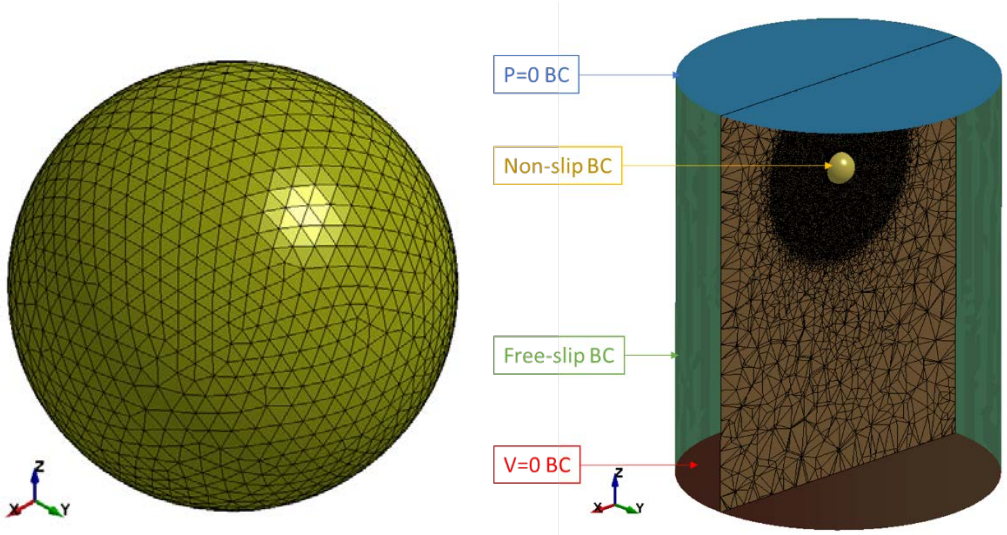

Figure 2: Reference test ball and domain description

The calculation shows a good mesher behaviour in its ability to follow the sphere. If elements quality deteriorates, automatic remeshing is triggered using *ICFD_CONTROL_ADAPT_SIZE, and if not remeshing frequency is considered every 50 steps.

Due to the unsteady flow and wake-building phase, the drag loads take time to reach expected values for a sphere. The next figure shows the computed vertical loads and a comparison with the drag curve for a smooth sphere as modelled by Clift, Grace and Weber [5]. The loads are nondimensionalized using the Reynolds number and the drag coefficient. It has to be noted that the Reynolds number range includes the critical regime for which the wake building and the boundary layer transition produce antagonistic effects on the loads.

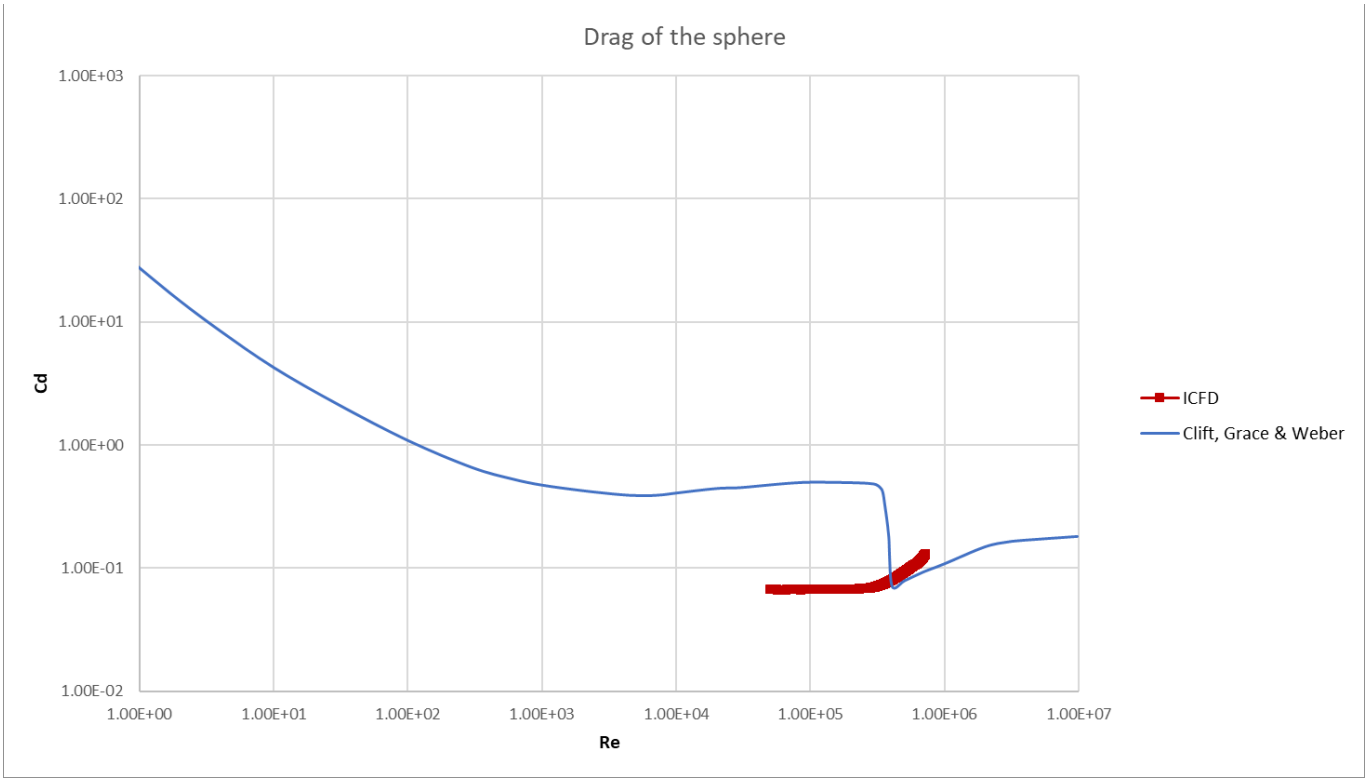

Figure 3: Drag loads of the free-falling sphere vs. steady flow experimental results

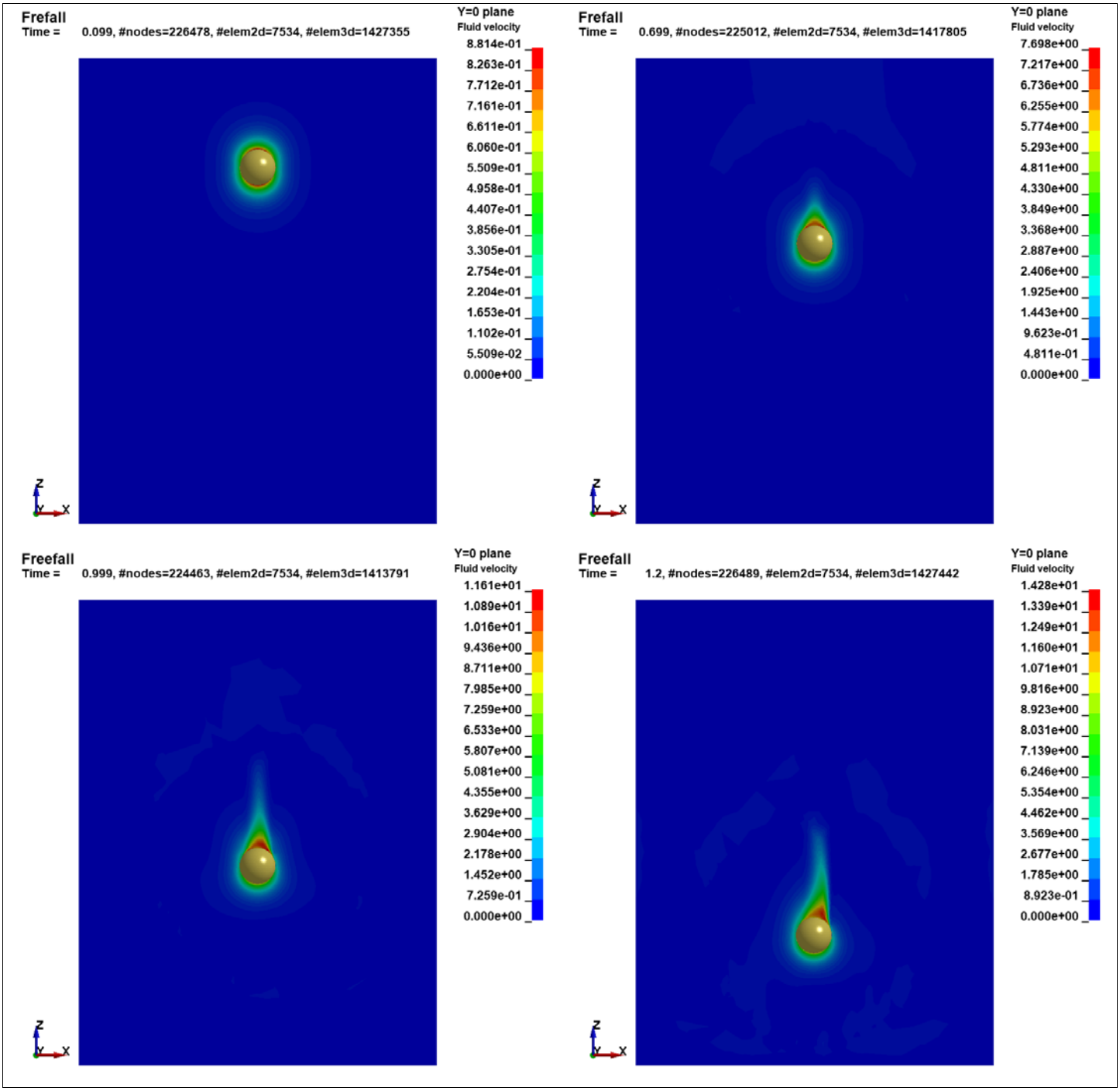

Figure 4: Velocity field at 100ms, 700ms, 1000ms and 1200ms

Validation of airdrop cases

Validation cases are selected based on works performed at the wind tunnel of DNW-NWB [6]. They consist in the ejection of a rectangular box from a transport plane model with an inflow velocity.

The preliminary methodologies are applied on the reproduction of these test cases. Three different payload weights are considered, and for the heaviest, three different inflow velocities are considered as well. These validation cases have a double interest:

- the flow is highly unsteady, with a null incident velocity when the payload is still in the cargo bay, up to Reynolds numbers of the order of 10^6 when the payload is clear from the plane and is fully in the velocity field: this covers a wide range of flow regimes around the box, including a translation and a rotation
- the nearly closed cargo bay permits to challenge the ICFD mesher, in particular in the interval between the payload and the ramp.

Because of the Froude scale adopted in the wind tunnel, Reynolds number ranges are significantly lower than at full scale. For this matter, additional sensitivity cases are run, in particular regarding the mesh size and the targeted y+ values at the payload surface. Comparisons are based on computed aerodynamical loads as well as payload trajectories. Although the computed trajectories tend to smooth out any discrepancies between test cases, they are representative of the phenomena of interest.

The payload consists in a 110x90x50mm block. Mass densities are respectively 120kg/m^3, 580kg/m^3, and 1000kg/m^3 for the light, medium and heavy payloads. Inflow velocities of 16m/s, 18m/s and 20m/s are applied with the heavy payload.

The cargo plane is a 1/26th model of a C17 Galaxy, with a wing span of 2m. The figure below shows the DNW-NWB model along with the payload ejection system.

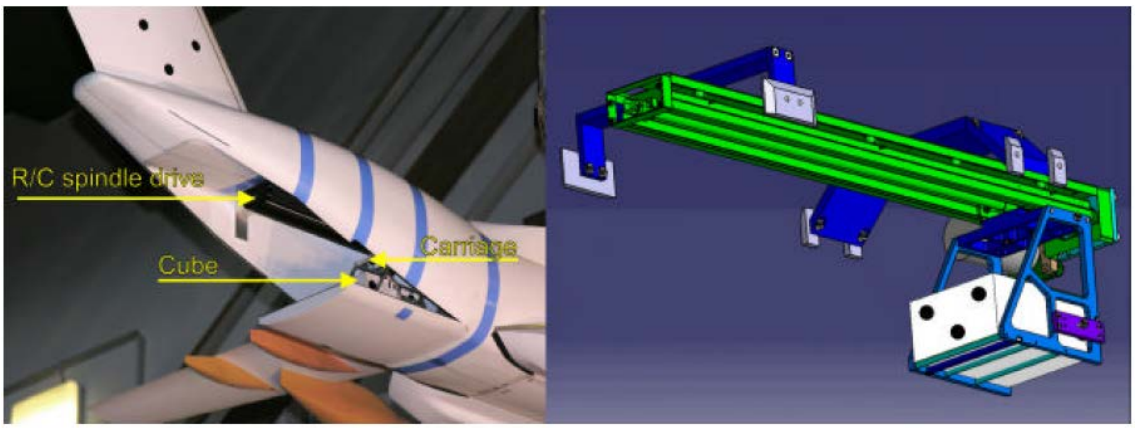

Figure 5: DNW-NWB wind tunnel model and payload ejection system

The ICFD model includes the external surfaces of both the plane and the payload as non-slip domain boundaries. The plane is meshed with 20mm triangles while the payload is meshed with 10mm triangles. A 5mm gap separates the payload and the plane exit ramp in order to allow the inclusion of fluid elements all around the payload. The domain is closed by a 10x6x3.5m box, with a $V=V_0$ inflow velocity, a P=0 outflow pressure, and a freeslip boundary condition on its peripheral surface. The surface is meshed with 200mm triangles.

The plane surface nose is located around 1 length downstream of the inflow surface, and its tail 2 lengths upstream of the outflow surface. The fluid mesh includes progressive boundary layer meshing on the plane and payload surfaces, with smallest mesh thicknesses of respectively 0.6mm and 0.3mm (NELTH=5 in *MESH_BL). Remeshing is triggered if element quality deteriorates, and otherwise every 50 cycles using *ICFD_CONTROL_ADAPT_SIZE.

The model can be seen in the following figures, along with a section plane on the longitudinal axis showing the initial fluid mesh.

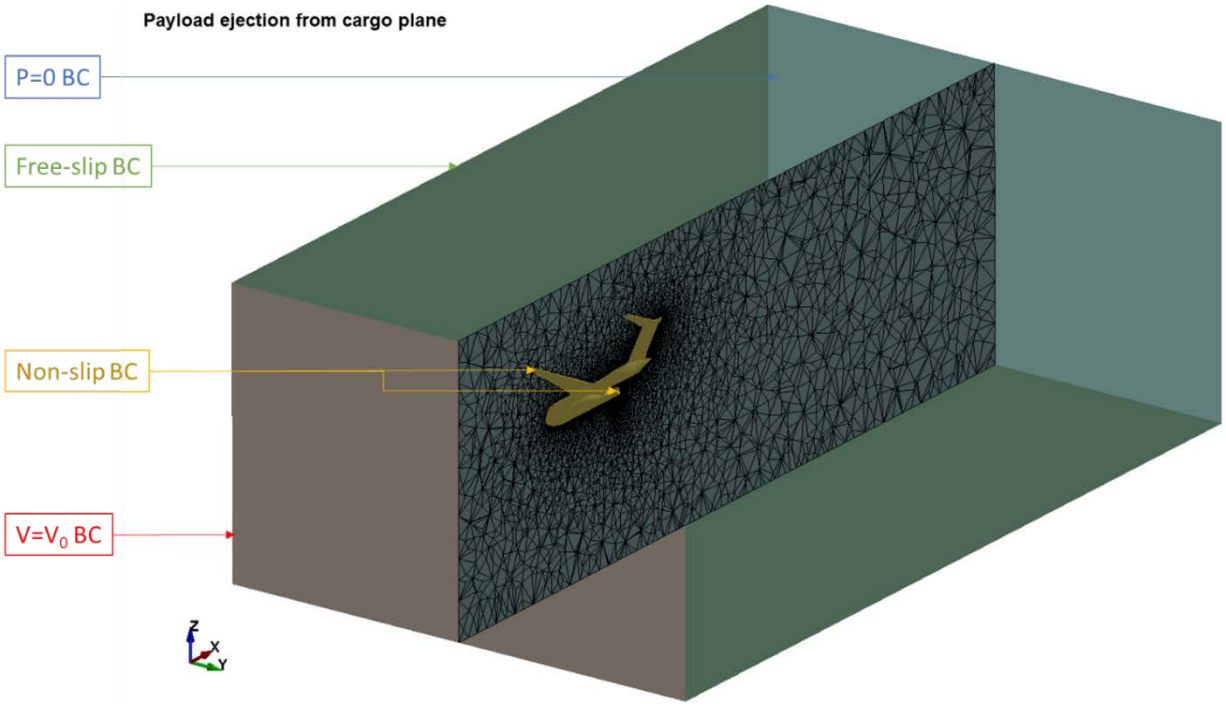

Figure 6: Airdrop model setup – domain definition

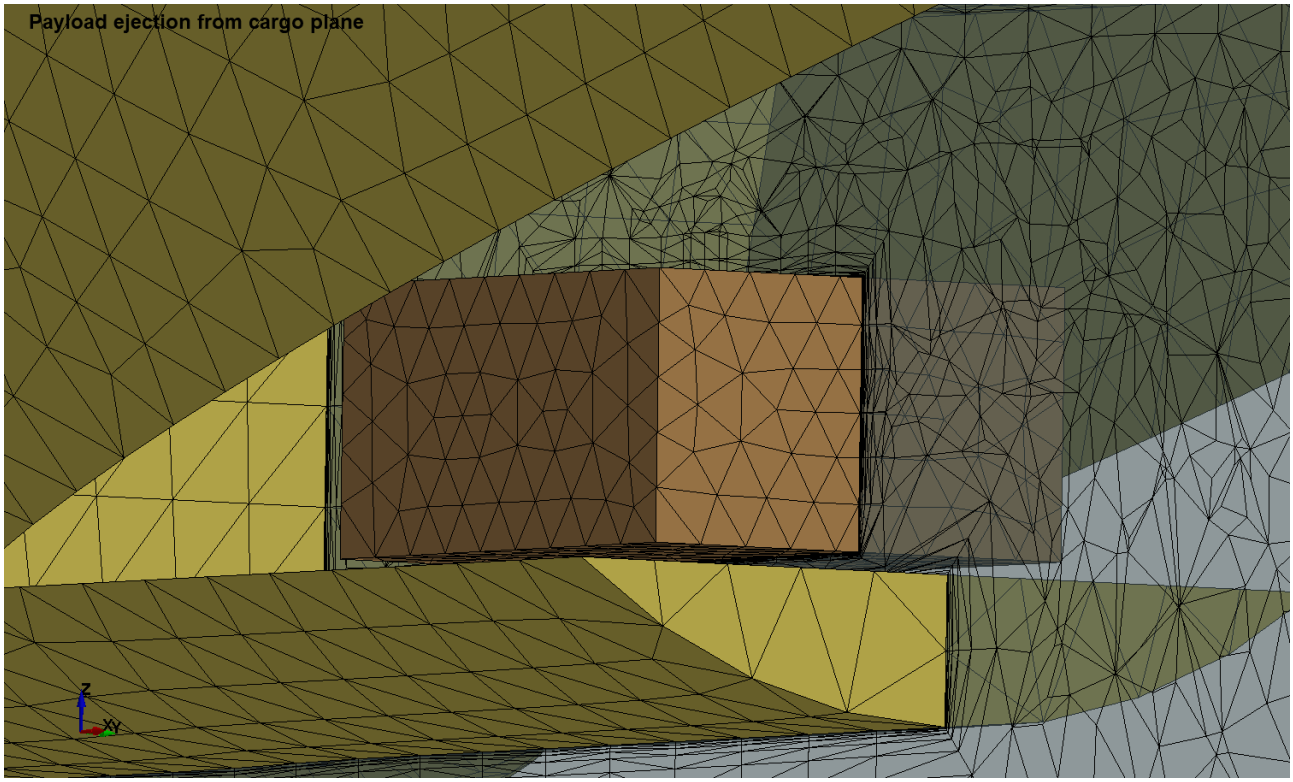

Figure 7: Airdrop model setup – close up on the payload initial position

First results and sensitivity study

The first case is run using the medium weight payload and the highest inflow velocity. Sensitivity analyses on the following parameters are performed:

- weak/strong coupling,
- LES/RANS turbulence model,
- standard/fine mesh size.

The reference case is run using weak coupling and a LES Smagorinsky turbulence model. The RANS model used for the test is the standard k-ε model with default tuning parameters.

The fine mesh uses 10mm triangles on the plane surface, and 8mm triangles on the payload surface. The boundary layer mesh is also considerably finer for the payload, with a thickness of the first element in the normal direction to the surface of 0.01mm.

The reference case shows quick computation times with only over 2 hours for almost 1 second of simulated time, with 28CPU in MPP. Structural and ICFD timesteps are the same, meaning the coupling loop does not have to interpolate the fluid loads during the ICFD cycles.

Although the initial fluid mesh contains 855,000 elements, the consecutive remeshings lower this number to around 560,000.

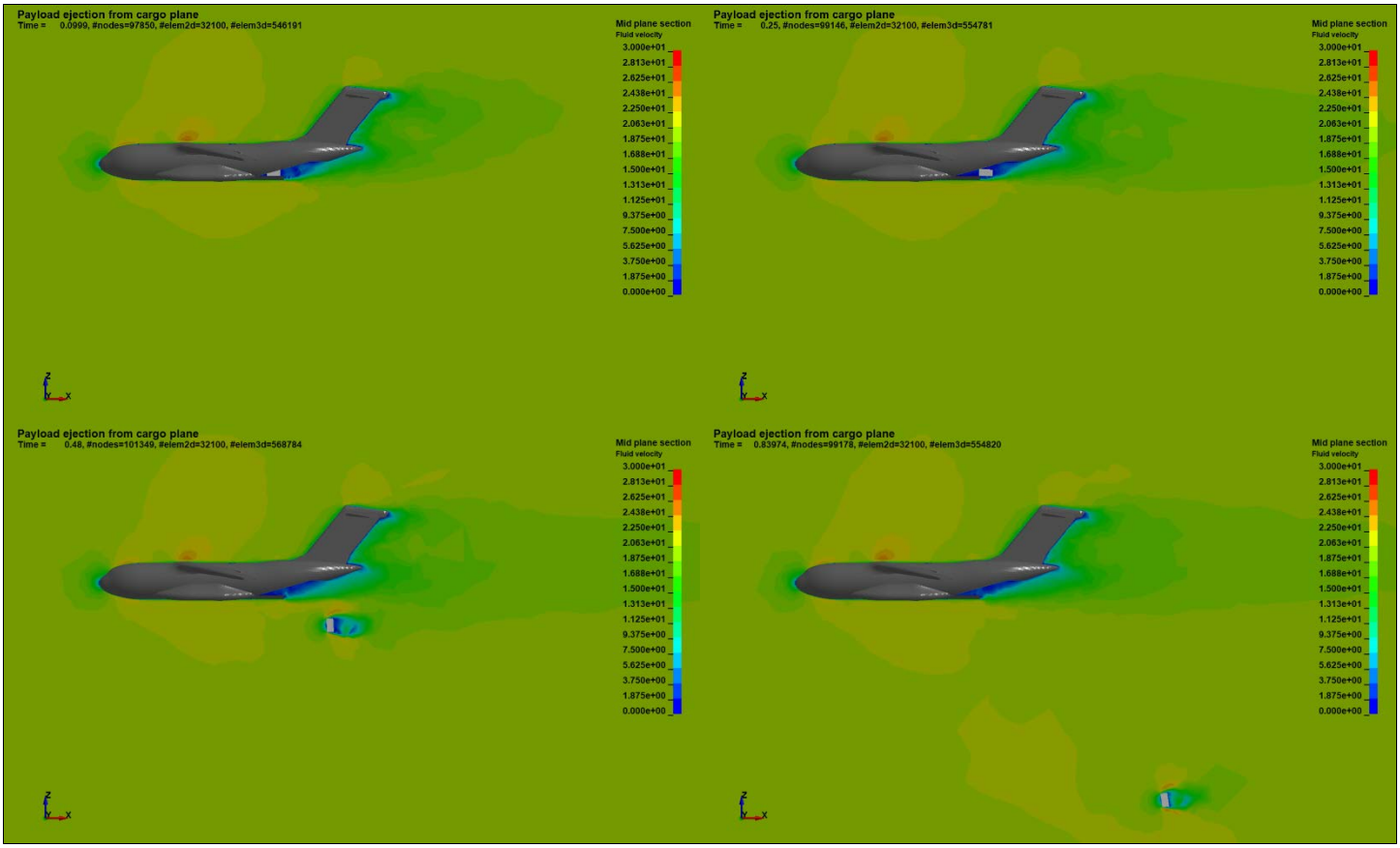

Figure 8: Airdrop simulation – velocity field at 100ms, 250ms, 480ms and 840ms

y+ values around the payload are lower than 25 at all times and locations. As this is significantly higher than the usually recommended value, the fine mesh results permit to assess the influence of the y+ on global loads.

The large payload density also permits to avoid instabilities due to added mass effects while using weak coupling. In addition, as the payload is a rigid body, forces transmitted by the fluid do not participate in structural deformations.

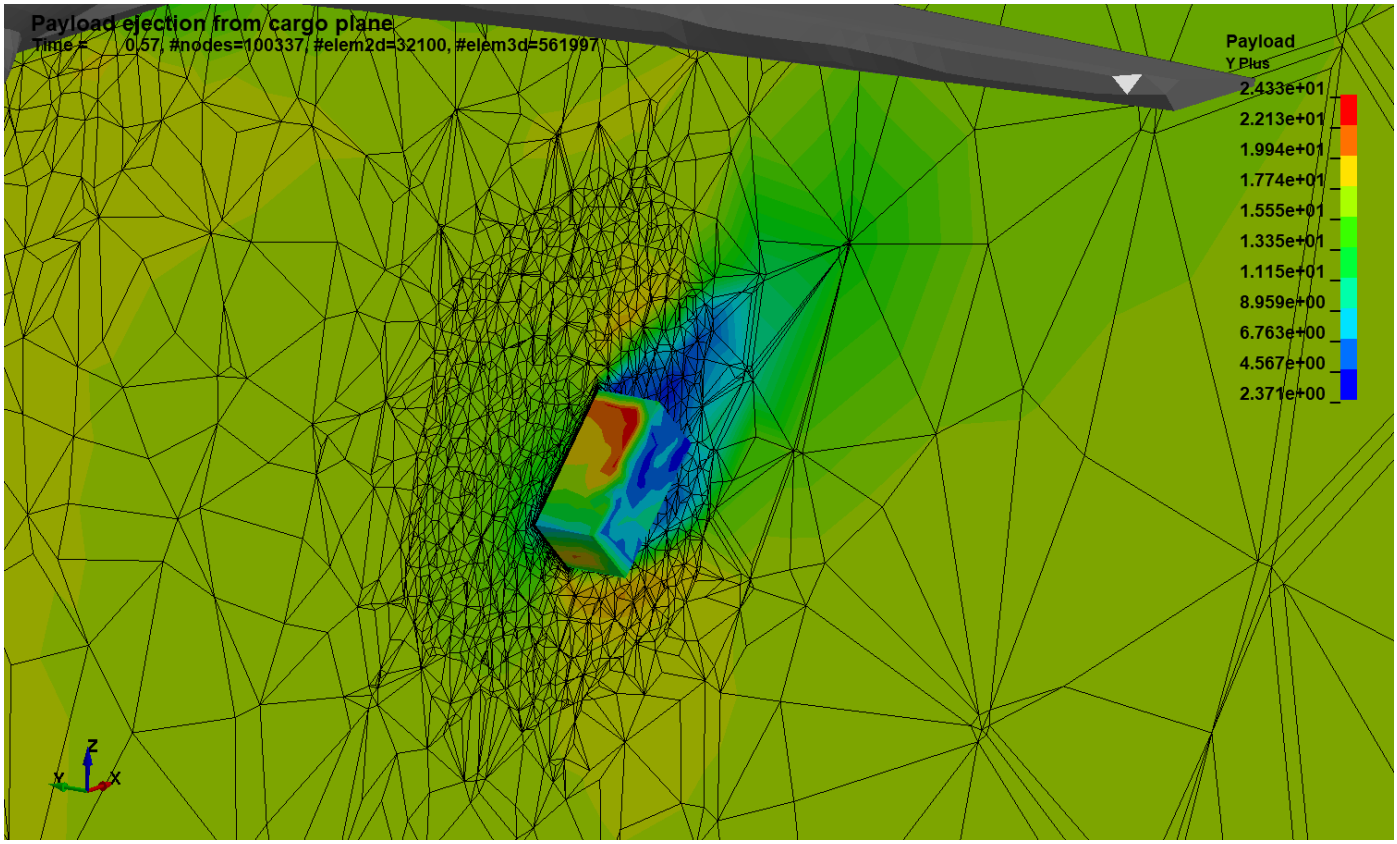

Figure 9: Airdrop simulation – maximum y+ value at 570ms

Computational times for the sensitivity cases are shown hereafter, up to 0.7s of simulated time. All cases were run with 28CPU in MPP. The reference case is more than three times faster than both the strong coupling and refined mesh cases.

Sensitivity case	CPU time (min)
Reference	105
Strong coupling	331
Refined mesh	342
RANS turbulence model	119

Table 1: CPU times for the sensitivity cases

The sensitivity results show a good agreement of the reference case with the refined mesh and the strong coupling, but not with the RANS turbulence model, as could be expected. This results in nearly identical trajectories for the three LES cases, while the vertical displacement with the RANS model is slightly off.

This sensitivity permits to validate choosing weak coupling with a relatively coarse mesh on the domain surfaces. This degradation of the calculation parameters leads to a similar payload behaviour for only a fraction of the computational cost.

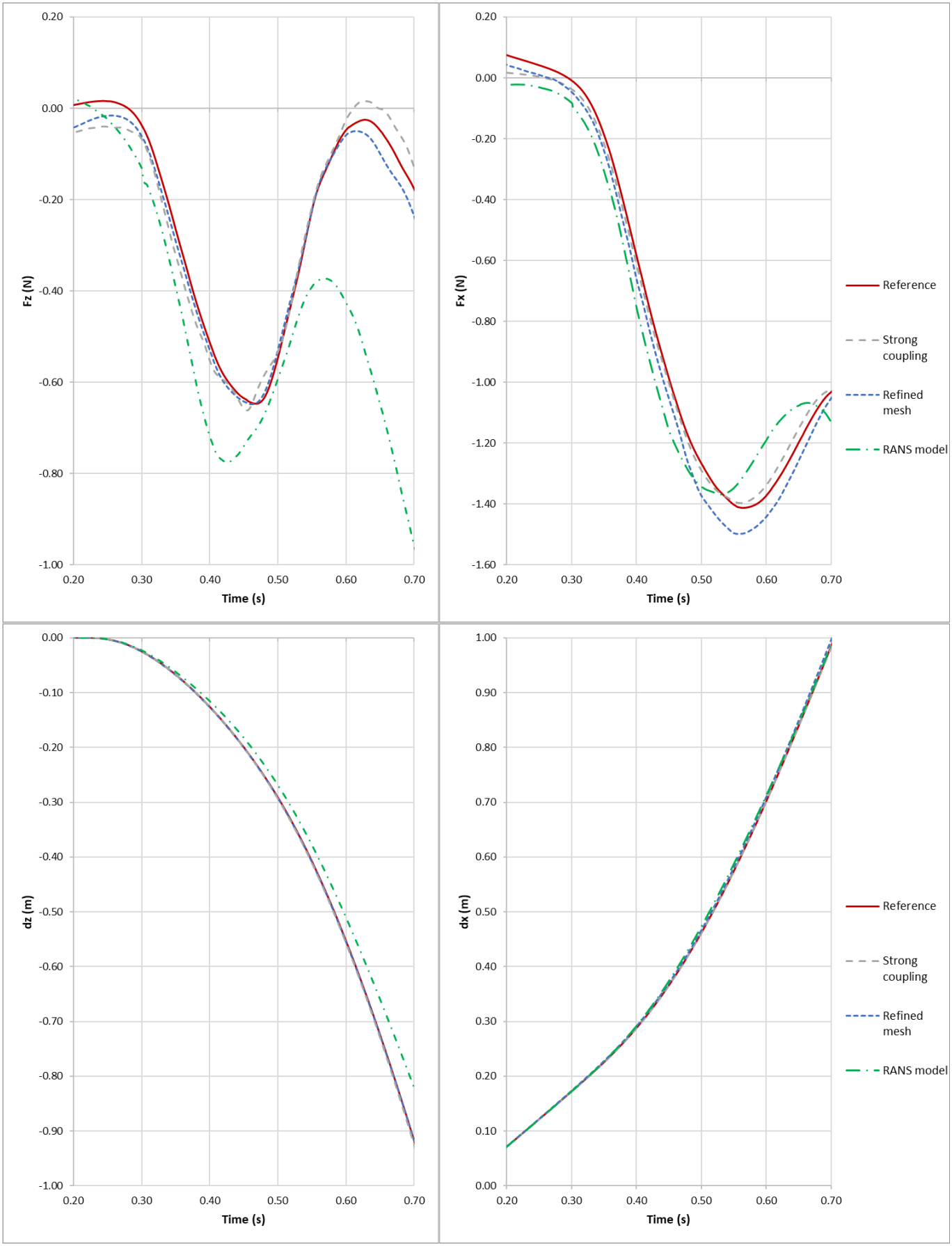

Figure 10: Loads (top) and trajectories (bottom) of the sensitivity cases

Validation cases

The drop test is adapted in order to reproduce the cases described in [6]. Although the reference paper describes a payload ejection velocity of 1m/s, first comparisons and extended analysis of the trajectories from the wind tunnel results show that the velocity needs calibration. An actual imposed velocity of 0.7m/s shows a good agreement with the experimental data at ejection, as can be seen on the initial slope of the horizontal displacements.

Results generally show a slight underestimation of the aerodynamic loads, particularly the horizontal force due to the inflow. However, trajectories are in very good agreement, especially when compared to those computed in the absence of air.

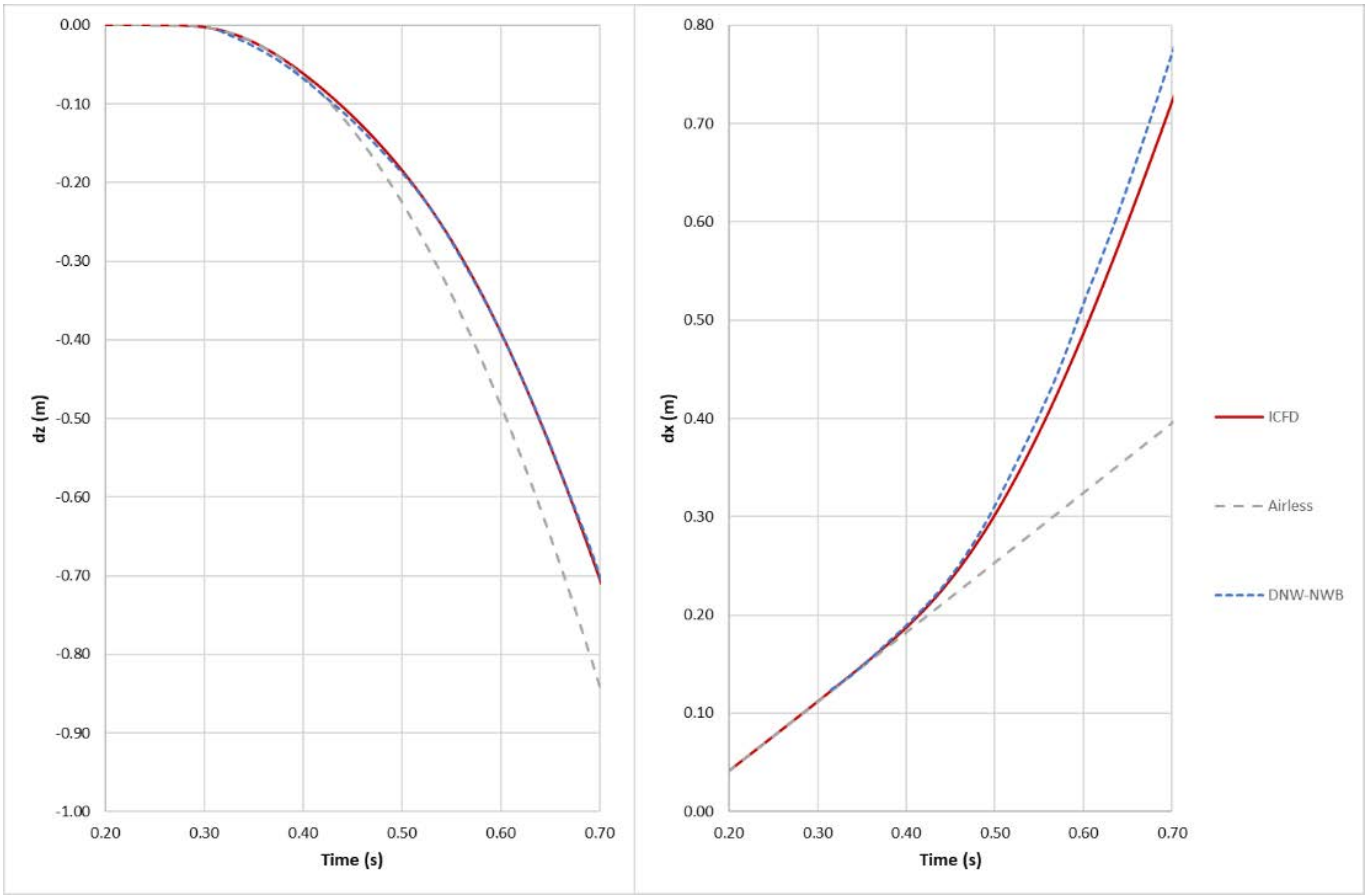

Figure 11: Validation case – trajectory of the medium payload

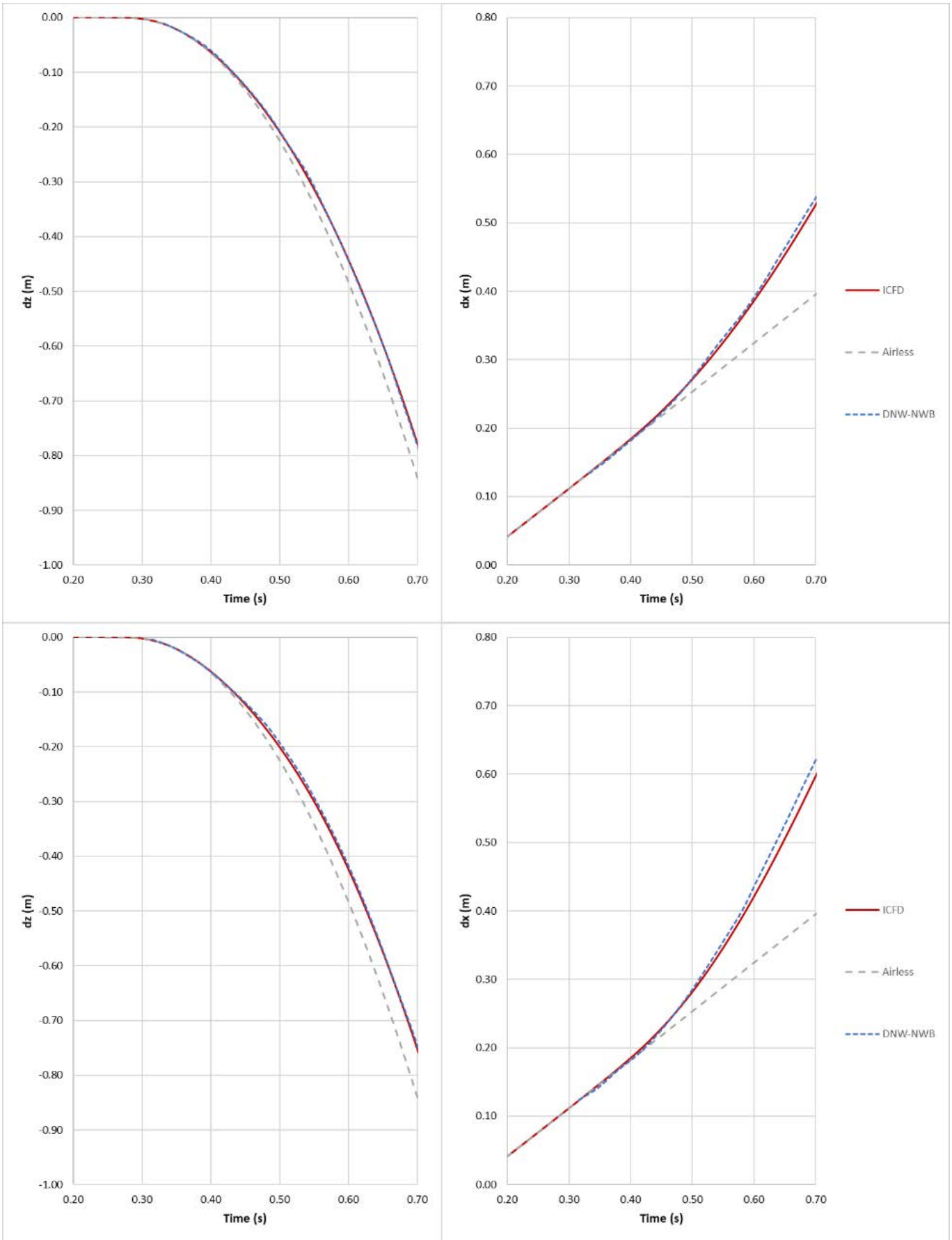

Figure 12: Validation case – trajectory of the heavy payload with a 16m/s (top) and 20m/s (bottom) inflow velocity

Snapshots of the freefall are also compared to experimental results. They reflect the quantitative observations already made about the horizontal and vertical displacements. Additionally, they also permit to assess the payload self-rotation, which is influenced by the air flow.

The light payload gets dragged into the eddies behind the plane and shows a chaotic behaviour. On the other hand, the medium and heavy payloads clear the disturbed area more quickly and the rotational positions are in agreement with the experimental runs.

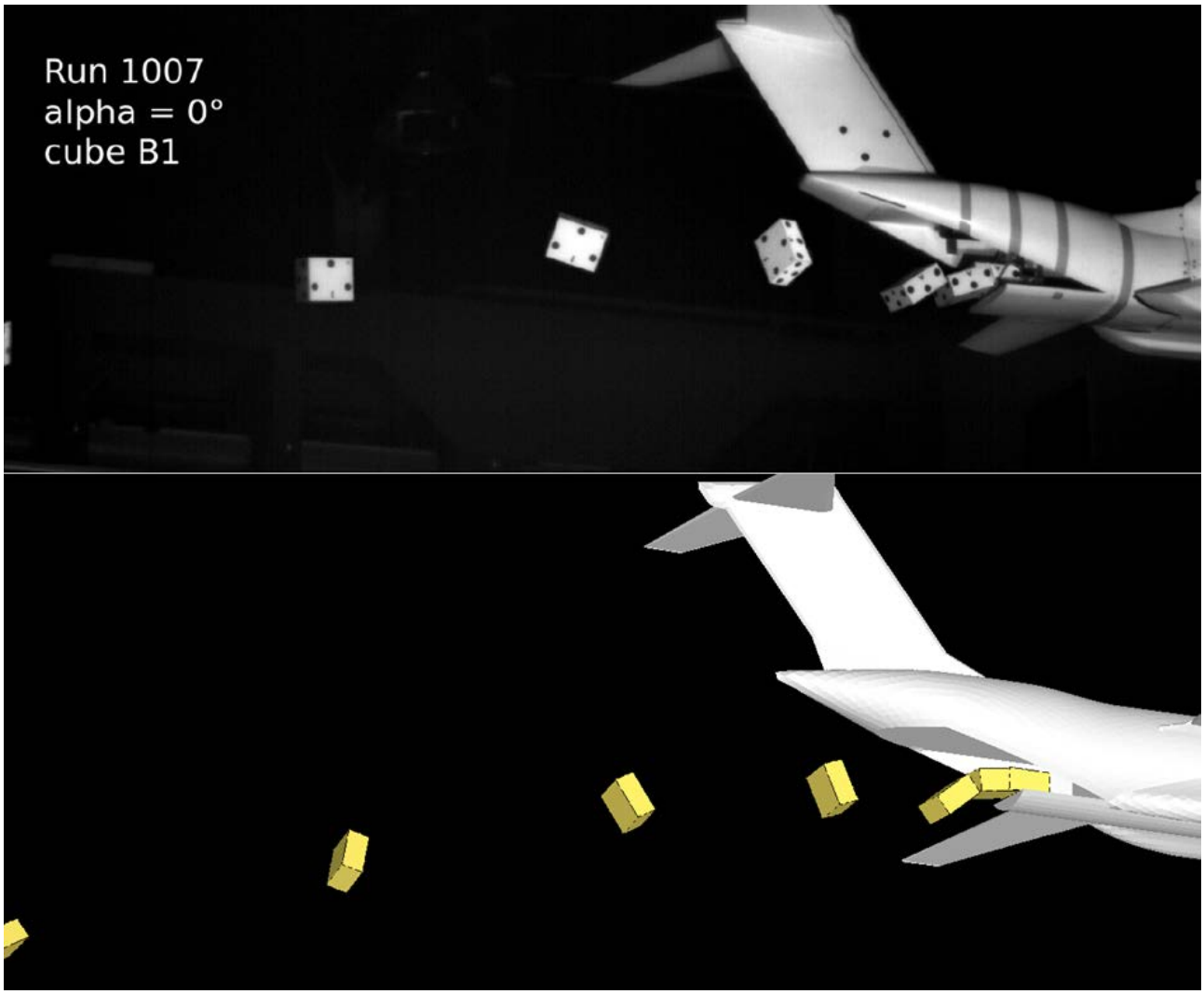

Figure 13: Validation case – successive snapshots of the light payload during freefall

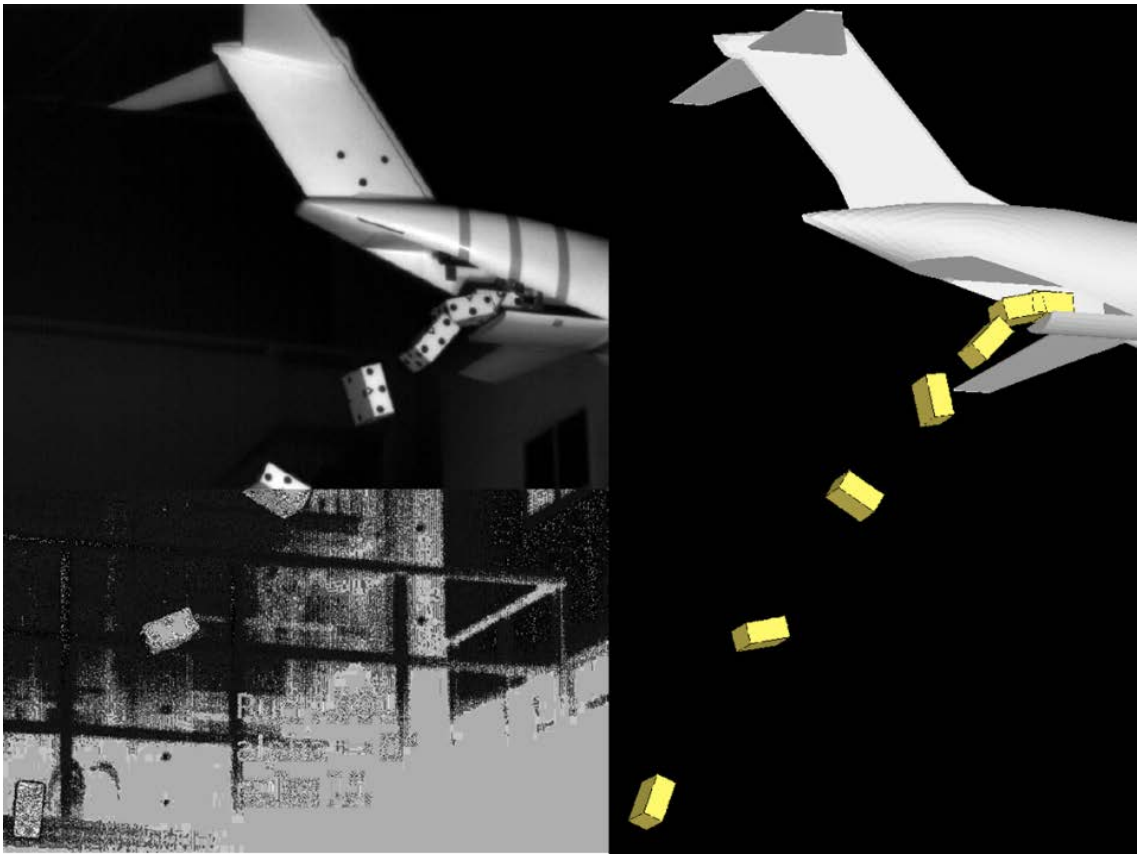

Figure 14: Validation case – successive snapshots of the medium payload during freefall

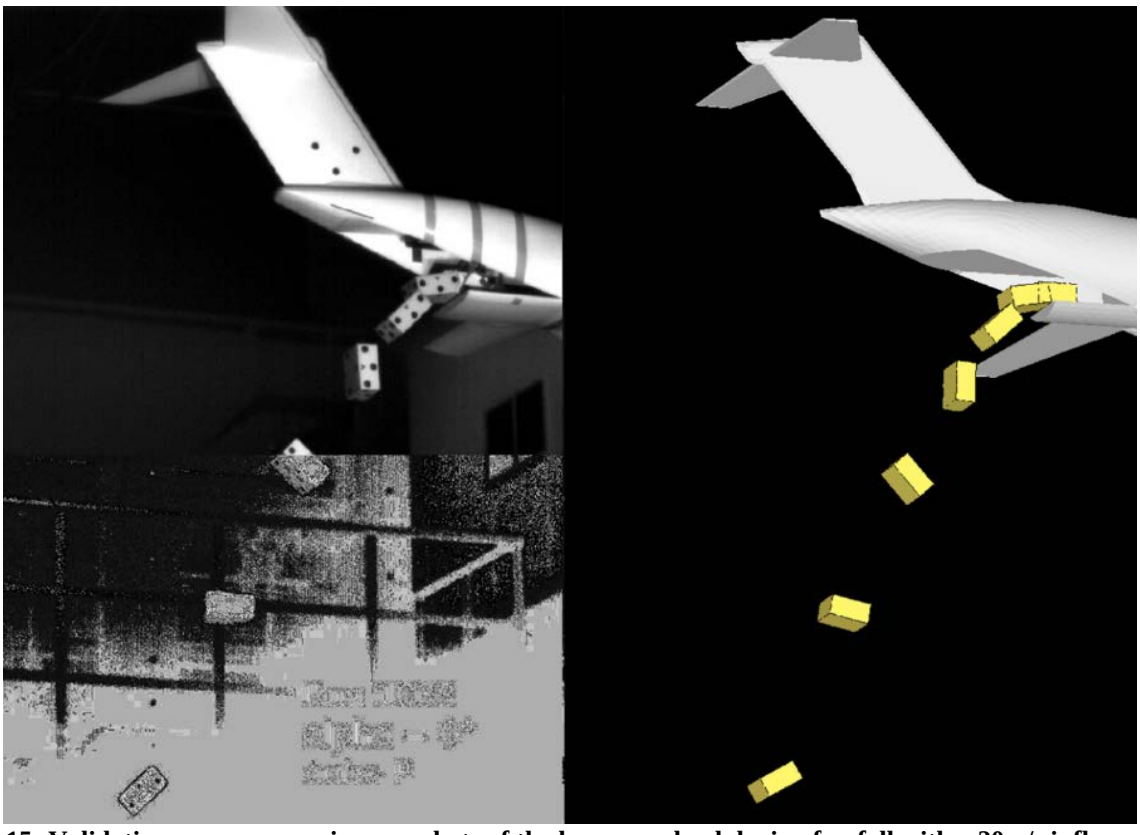

Figure 15: Validation case – successive snapshots of the heavy payload during freefall with a 20m/s inflow velocity

Additional sensitivity analyses are run in order to identify the source of the observed discrepancies. An inflow velocity of 21m/s is considered, as well as an air density of 1.25kg/m^3. Although the increase of 2% in air density does not lead to significant changes, an increase of 5% in wind tunnel velocity shows a large influence on the observed trajectories. As the exact calibration of the air velocity in the DNW-NWB wind tunnel was not disclosed in their paper, the predicted trajectory of the ICFD calculations could be in the approximation range.

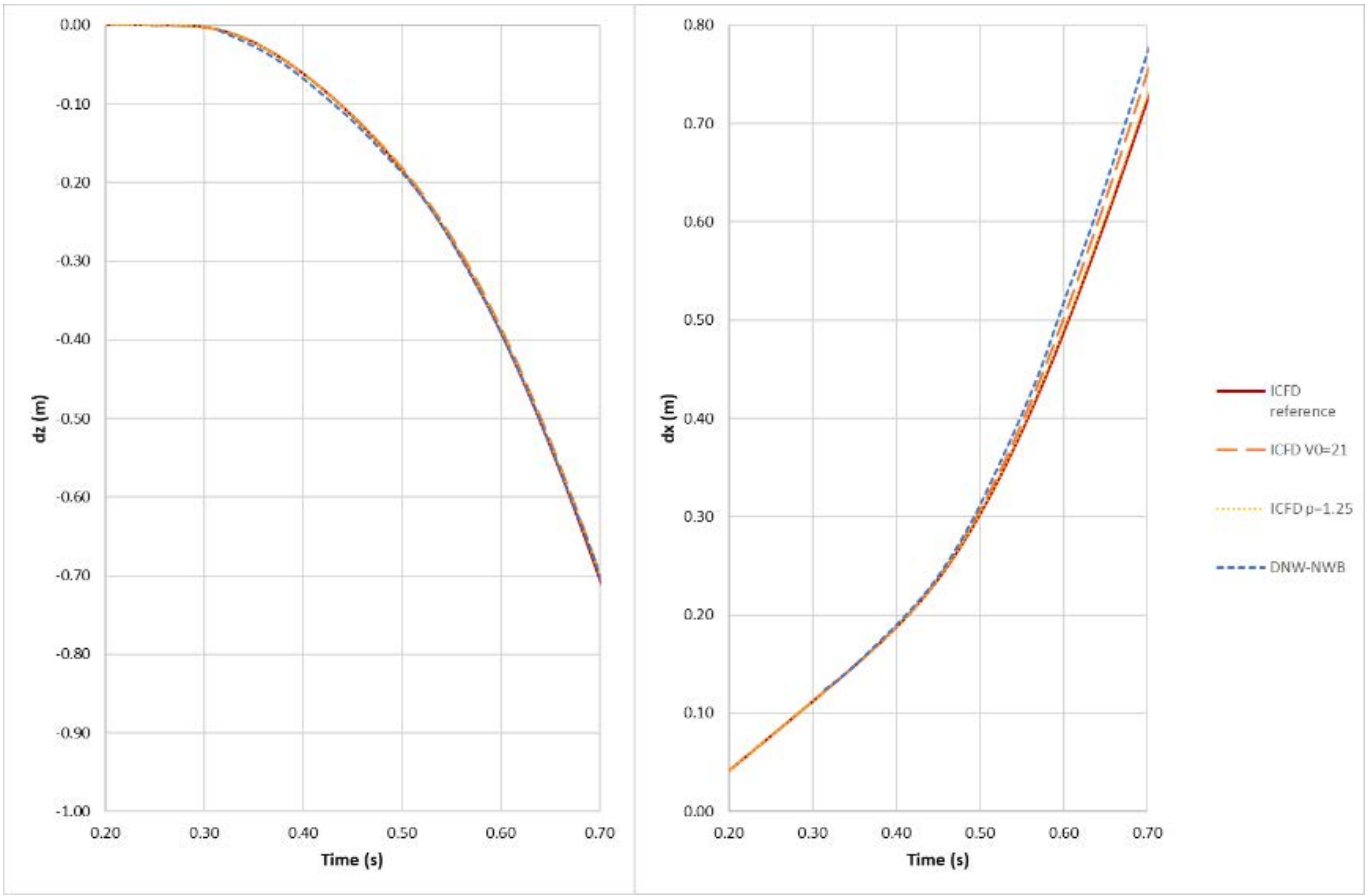

Figure 16: Validation case – sensitivity on the air flow parameters

Conclusion and perspectives

The present work permits to demonstrate the ICFD mesh robustness, whether for the mesh movement while following a moving boundary or full remeshing when necessary. New refining tools have also been successfully tested, allowing selectively refined zones to follow the objects of interest while keeping a coarse mesh in the rest of the domain. This enables to reduce significantly the CPU time.

Aerodynamic loads have shown good accuracy despite the choices of a coarse mesh and only a weak coupling strategy, which also permitted to reduce CPU time. The validation cases have been successfully reproduced, with good trajectory predictions.

The next step of PARAFLU project will now consist in modelling the parachute deployment. The new ICFD features will be of great help. However, strong coupling will be necessary because of the low parachute mass and its high deformability.

Acknowledgements

The authors wish to thank the LSTC ICFD development team, especially Rodrigo Paz, Facundo Del Pin and Iñaki Çaldichoury for their involvement and the various new tools available in the ICFD solver.

This work was realized as part of a RAPID project financed by the French Government in order to improve parachutes simulation with LS-DYNA.

References

[1] Coquet Y., Bordenave P., Capmas G., Espinosa C., *Improvements in fluid structure interaction simulation of parachute using LS-DYNA*, 21st AIAA, 2011-2590.

[2] Tutt B., Charles R. D., Roland S., Noetscher G., *Development of parachute simulation techniques in LS-DYNA*, 11th International LS-DYNA Users Conference, 2012.

[3] McQuilling M., Potvin J., Riley J., *Simulating the Flows About Cargo Containers Used During Parachute Airdrop Operations*, 28th AIAA Applied Aerodynamics Conference, Chicago, IL, June 28 - July 1, 2010

[4] Desabrais K. J., *Aerodynamic Forces on an Airdrop Platform*, 18th AIAA, 2005-1634.

[5] Clift R., Grace J.R. and Weber M.E., *Bubbles, drops and particles*, Academic Press, 1978

[6] Loeser T., Bergmann A., *Capabilities of Deployment Tests at DNW-NWB*, Fluid Dynamics of Personnel and Equipment Precision Delivery from Military Platforms (pp. 10-1 to 10-12), 2006

[7] Michel C., Grippon E., Seulin M., Lapoujade V., *Freefall movement decomposition of a payload released by aircraft: study of aerodynamic coefficients using the LS-DYNA ICFD solver*, 11th European LS-DYNA Conference, 2017